Orientational Order of Molecular Assemblies on Inorganic Crystals

D. A. Saville,[1] J. Chun,[1] J.-L. Li,[2] H. C. Schniepp,[1] R. Car,[2] and I. A. Aksay[1]

[1]*Department of Chemical Engineering, Princeton University, Princeton, New Jersey 08544, USA*
[2]*Department of Chemistry, Princeton University, Princeton, New Jersey 08544, USA*

Surfactant micelles form oriented arrays on crystalline substrates although registration is unexpected since the template unit cell is small compared to the size of a rodlike micelle. Interaction energy calculations based on molecular simulations reveal that orientational energy differences on a molecular scale are too small to explain matters. With atomic force microscopy, we show that orientational ordering is a dynamic, multimolecule process. Treating the cooperative processes as a balance between van der Waals torque on a large, rodlike micellar assembly and Brownian motion shows that orientation is favored.

Self-assembling surfactant micelles and proteins are of interest in the molecular level processing of materials with nanoscale structural design. Because of the fact that self-assembly involves multiple nucleation sites, the process often needs to be guided to control the structure at microscopic and larger length scales. Inorganic single crystals have been used as templates to guide the self-assembly of micelles and proteins with order that reflects the underlying crystal structure, although the reasons for the ordering are uncertain [1–5].

Orientational order on crystals has been studied in a variety of nonmicellar systems where it has been called epitaxy [6], quasiepitaxy [7], and van der Waals epitaxy [8]. However, Wanless and Ducker [9] demonstrated that the spacing of cylindrical micelles on a highly ordered pyrolytic graphite (HOPG) substrate is not an integer multiple of the graphite unit cell which excludes epitaxy as the governing mechanism. Forrest [10] reviewed the potential energy calculation basis of orientation for organic thin films where, to simplify matters, the adlayer energies of adjacent molecular units were lumped into simpler entities interacting with the substrate. Although this formalism yields the orientation from the minimum energy configuration, Forrest cautions that, in practice, ordering depends on the nonequilibrium conditions under which a film grows. Because potential energy minimization can be computationally intensive, geometrical lattice misfit algorithms have been developed [11,12]. Such methods are not successful with certain configurations since they do not account for the relative strengths of adsorbate-substrate interactions and are not applicable to long, linear molecules or rodlike assemblies. None of these methods is appropriate for surfactant adsorption for several reasons, e.g., the role of the water solvent is omitted and the fact that molecules access a large number of configurations at nonzero temperatures.

This Letter describes a study of the orientational order of a molecular assembly adsorbed on graphite in an aqueous environment. The micelle assembly is composed of surfactant molecules of cationic cetyltrimethyl ammonium chloride (CTAC) (with micelle diameters ∼10 times the crystal lattice size) spanning hundreds of lattice units of the template—HOPG. Using liquid-cell atomic force microscopy (AFM) in the double layer repulsion mode, it was previously shown that these micelles align with respect to the underlying HOPG crystal [1–4]. We confirmed the alignment with the underlying structure in our experiments. Then, using the same technique, we acquired the sequence of deflection images (Fig. 1) showing the dynamic competition between grains of two different orientations, β and β'—the small difference in contrast between the two grains is most likely caused by an asymmetry of the AFM probe.

This dynamic behavior—not addressed in previous AFM studies [1–5]—prompts us to propose a mechanism where micelles continuously disintegrate and reform while retaining their orientational order along the β, β', or β'' axes of the graphite crystal. This scenario is also in line with the continuous exchange of surfactants between micelles and bulk solution at small time scales [13]. To interpret this behavior, we model the system at two length scales, molecular and colloidal. At the molecular level, we investigate interaction energy differences between different orientations for a single molecule. These are too small to explain ordering so we move to a larger length scale to investigate orientational ordering in terms of an anisotropic van der Waals interaction. At the colloidal level, we demonstrate that a van der Waals torque on the assembly results from collective effects on the larger length scale. This formalism leads to orientation, bridges the length scales, and accounts for temperature effects.

To examine the behavior of individual surfactant molecules at the molecular scale, van der Waals interaction energies are computed for CTAC adsorbed on HOPG. First, for a given orientation, we use a standard density-
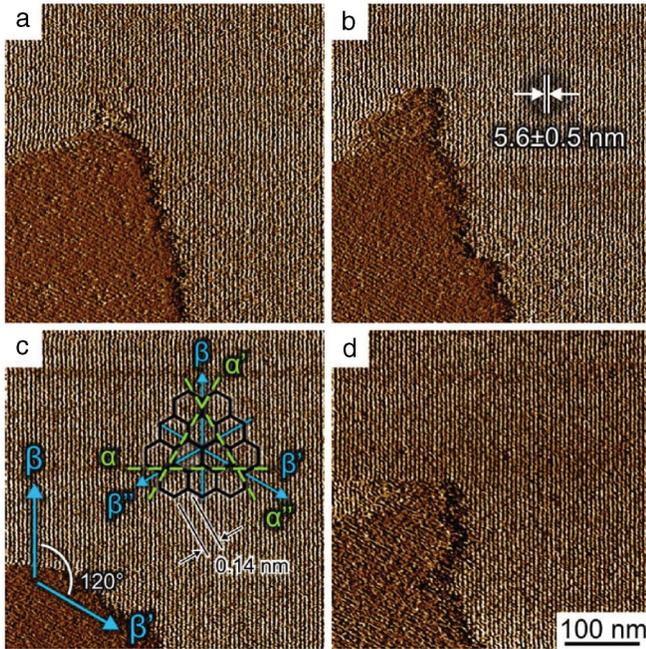
FIG. 1 (color online). 500×500 nm AFM images—acquired at a scan rate of about 7 lines/s—of hemicylindrical surfactant aggregates formed on HOPG in a 10 mM CTAC solution. Images (a)–(d) show the same area at intervals of 70 s. After reaching thermal equilibrium, the drift is less than 1 nm per min and time-lapse imaging of a given region is possible. Panel (c) also defines the three α and the three β directions, parallel and perpendicular to the symmetry axes of graphite. A MultiMode/NanoScope IIIa AFM, Veeco Instruments, Santa Barbara, CA, was used.

functional theory calculation to optimize the geometry such that the surfactant is in "contact" with graphite surface. Figure 2 shows two perpendicular CTAC orientations, α (left) and β (right) directions, parallel and perpendicular to symmetry axis. To mimic the hydrophobic interaction that keeps the surfactant near the HOPG surface in an aqueous solution, a uniform external force (1.65×10^{-10} J/m) is applied on each carbon atom of the CTAC hydrophobic tail. The force is estimated from the hydrocarbon surface tension parameter in water [14]. The relaxation process gives an average separation of about 0.35 nm. Finally, the van der Waals interaction between the CTAC surfactant and graphite is calculated by empirical atom-atom molecular-mechanics simulations and pairwise summation over the attractive part of Lennard-Jones potentials [15] between CTAC and graphite. Figure 2 shows van der Waals energies of CTAC on graphite calculated for several positions with the same orientation. Given that the underlying electron densities of the graphite are different for two orientations, the resulting van der Waals interaction is anisotropic. As shown in Fig. 2, the van der Waals energy difference between the two orientations is about 22 meV, comparable to the thermal energy,
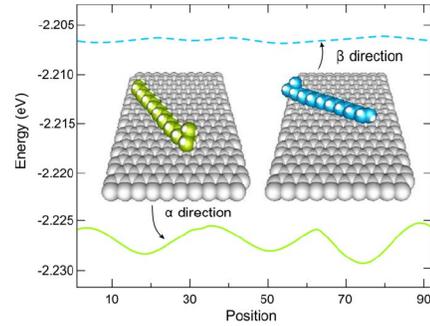

FIG. 2 (color online).   Diagrams: A CTAC molecule lying parallel to a symmetry axis of graphite, α orientation (left). The β orientation (right) is perpendicular to the symmetry axis on the same graphite surface. Curves: Calculated van der Waals energies of the molecule on a graphite surface. The atoms are represented by their respective van der Waals radii. The molecule was moved laterally on the graphite surface so as to sample different positions with the same orientation. The energetic difference between two orientations is about 22 meV. Note that adsorption of surfactant in the α orientation corresponds to micelle alignment in β orientation; thus the constituent molecules of a micellar hemicylinder are oriented perpendicular to its axis.

$kT(\sim 26 \text{ meV})$. However, this small energy difference is unlikely to explain the orientational ordering and, due to temperature effects, the energy of a surfactant assembly is not an additive property that can be computed from the behavior of a single molecule. So, without doing a full computationally prohibitive molecular dynamics simulation, there is no simple way to determine the collective effect of adding individual surfactants.

To investigate behavior at the micellar (colloidal) length scale, a simpler approach is needed and we chose to view a micelle as a macroscopic "rod," parallel to the surface of an underlying crystal. Accordingly, the rod represents an assembly of many molecules, and the overall interaction depends on the orientation of the rod with respect to the symmetry axes of the substrate and the separation between the substrate and the rod. To calculate the most probable orientation and include thermal motion, we balance van der Waals forces against Brownian forces as follows.

Using the Lifshitz theory set out by Parsegian and Weiss [16], the anisotropic van der Waals interaction between a dielectrically isotropic cylindrical rod and anisotropic semi-infinite slab in an isotropic medium was calculated [17,18]. Then the interaction between a hemicylindrical rod of length, l, and radius, a, and an anisotropic substrate can be written as

$$U(R, \theta) = -\frac{A_H^{\text{aniso}}(\theta)a^2 l}{6(h-a)^3}, \quad (1)$$

where the anisotropic Hamaker constant A_H^{aniso} is

$$A_H^{\text{aniso}} = \frac{3}{4}kT\sum_{n=0}^{\infty}{}' \int_0^{\infty} dx\, x e^{-x} \frac{(\varepsilon_m - \varepsilon_r)}{[\varepsilon_m + (\varepsilon_\beta \varepsilon_z)^{1/2}]^2} \left[\frac{(47\varepsilon_m^2 + 14\varepsilon_m\varepsilon_r + 3\varepsilon_r^2)(\varepsilon_m^2 - \varepsilon_\beta\varepsilon_z)}{8\varepsilon_m(3\varepsilon_r + \varepsilon_m)(\varepsilon_r + 3\varepsilon_m)} - (\varepsilon_\beta\varepsilon_z)^{1/2} \frac{\varepsilon_m}{3\varepsilon_r + \varepsilon_m}\left(\frac{\varepsilon_\alpha - \varepsilon_\beta}{\varepsilon_\beta}\right) \right.$$

$$\left. + \frac{(1 + 2\cos^2\theta)}{16}\left(\frac{\varepsilon_\alpha - \varepsilon_\beta}{\varepsilon_\beta}\right)\frac{(\varepsilon_m - \varepsilon_r)}{2(\varepsilon_r + 3\varepsilon_m)}(\varepsilon_\beta\varepsilon_z)^{1/2} \right]. \tag{2}$$

Here h is the separation between the hemicylindrical rod and the surface, and ε_m and ε_r denote the dielectric functions of medium (water) and rod. The $(h - a)$ distance arises because the interaction calculation uses a "composite" rod; i.e., half is a hemicylindrical hydrocarbon rod and the other half is water. Note that in this expression ε_α and ε_β are the dielectric functions in the plane of the surface, and ε_z represents the dielectric function perpendicular to surface. In addition to the frequency summation for n, a wave vector integration was performed; $x(\equiv 2qh)$ and q denotes the magnitude of the wave vector. The prime in the summation indicates that the $n = 0$ term is to be multiplied by 1/2. Special attention was given to short wavelength contributions [18] so as to obtain the full anisotropic character of graphite. Note that the anisotropic Hamaker constant depends on θ, the angle between the axis of the rod and a symmetry axes of a substrate, as indicated in Fig. 3.

To describe rotational motion parallel to the surface by the anisotropic van der Waals interaction, we use a Smoluchowski equation [19] for the equilibrium orientation probability distribution function, ψ. At equilibrium in a quiescent system,

FIG. 3. The relative probability relation for hemicylindrical micelles ($a = 2.0$ nm) of different lengths adsorbed on graphite in water. The inset is a schematic orientation diagram. Here x and y denote distances parallel and perpendicular to one of the symmetry axes of HOPG. The orientation of the rod is given by the director, **p**, lying parallel to the long axis of the assembly. A large relative probability represents a strong tendency for alignment perpendicular to the symmetry axis of the graphite.

$$\frac{\partial \ln\psi}{\partial \mathbf{p}} = -\frac{1}{kT}\frac{\partial U}{\partial \mathbf{p}}. \tag{3}$$

Here U denotes the anisotropic van der Waals interaction, and **p** is a unit vector denoting orientation. Accordingly, the balance between torques associated with Brownian motion and the van der Waals interaction establishes the orientation probability distribution of the assembly. For rotational motion in the xy plane, it suffices to consider one component of Eq. (3), and the probability density function $f(p_x)$, after normalization, is

$$f(p_x) = \frac{\exp(-\frac{\hat{A}}{2}p_x^2)}{\int_0^1 d\tilde{p}_x \exp(-\frac{\hat{A}}{2}\tilde{p}_x^2)}, \tag{4}$$

with $\hat{A} = A'\frac{a^2 l}{6(h-a)^3}$. A' is obtained from differentiation of the anisotropic Hamaker constant with respect to p_x and scaled on kT. Clearly the probability density becomes uniform for isotropic substrates where $\hat{A} = 0$. For $\hat{A} > 0$, the probability is a maximum for $p_x = 0$ (where rods are aligned perpendicular to the symmetry axis) and a minimum at $p_x = 1$. The relative probability ratio of the two orientations is

$$\tilde{\gamma} = \frac{P_{\text{perpendicular}}}{P_{\text{parallel}}} = \exp\left(\frac{\hat{A}}{2}\right), \tag{5}$$

where P_{parallel} and $P_{\text{perpendicular}}$ denote probabilities for parallel and perpendicular configurations of the rod, respectively. Equation (5) establishes a simple, quantitative relationship between the energy and the orientational order, at equilibrium, and predicts the degree of orientational ordering given parameters such as the dielectric properties and geometrical factors.

For hemicylindrical micelles on HOPG in an aqueous solution, the series representation for the Hamaker function A_H^{aniso} was summed into ultraviolet region ($\sim 10^{17}$ rad/s). For ε_m and ε_r, the dielectric response functions of water and hydrocarbon [20] are incorporated in the calculation along with the full dielectric response in terms of frequency and wave vector dependence for graphite [18]. Using the dielectric functions, we calculated the dimensionless torque parameter A' for a hemicylindrical micelle interacting with graphite across a thin film of water. Although A' is small, 1.991×10^{-5}, the relevant quantity is $\hat{A}$, which can be substantial for long rods close to the surface. Figure 3 depicts the relative probability as a function of separation and assembly size. The relative probability increases significantly as the separation decreases, which indicates that the preferred orientation of
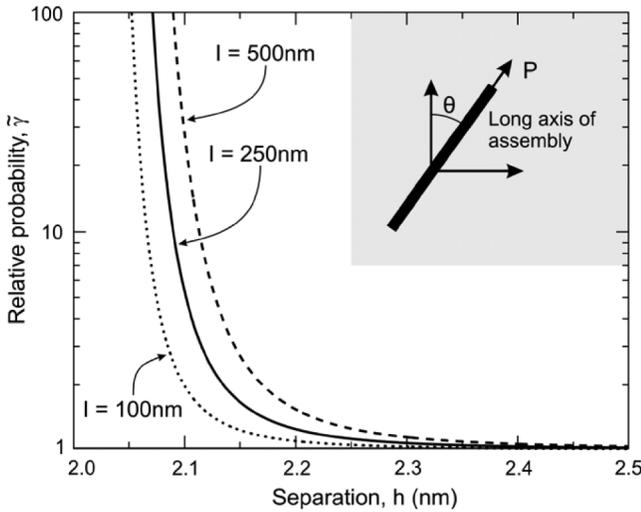
the micelle is perpendicular to the symmetry axis of graphite in accord with our experiment. In addition, the tendency for orientational ordering becomes significant as the assembly size increases, which can be understood as a collective effect due to the assembly of surfactant molecules. The formulation provides the relationship between the energy and orientational order using geometrical factors and physical properties.

Although our colloidal approach provides a satisfactory interpretation for the origin of orientational order, it still needs improvement. In its present form, (i) it cannot handle the dynamic nature of the micelle disintegration and reassembly, (ii) it treats the micelle as rigid rods instead of flexible entities, and (iii) the micellar rods are noninteracting. In spite of these deficiencies, the equilibrium orientational order by anisotropic van der Waals interaction and resulting torque capture the process at the colloidal level; the torque leads to a minimum energy configuration of molecular assembly. In addition, since the torque is dependent on the size of molecular assembly, small energy differences at the molecular scale are thereby assembled into a collective effect.

[1] S. Manne, J. P. Cleveland, H. E. Gaub, G. D. Stucky, and P. K. Hansma, Langmuir **10**, 4409 (1994).

[2] S. Manne and H. E. Gaub, Science **270**, 1480 (1995).

[3] I. A. Aksay, M. Trau, S. Manne, I. Honma, N. Yao, L. Zhou, P. Fenter, P. M. Eisenberger, and S. M. Gruner, Science **273**, 892 (1996).

[4] H. N. Patrick, G. G. Warr, S. Manne, and I. A. Aksay, Langmuir **13**, 4349 (1997).

[5] C. L. Brown, I. A. Aksay, D. A. Saville, and M. H. Hecht, J. Am. Chem. Soc. **124**, 6846 (2002).

[6] M. Hara, H. Sasabe, A. Yamada, and A. F. Garito, Jpn. J. Appl. Phys. **28**, L306 (1989).

[7] F. F. So and S. R. Forrest, Phys. Rev. Lett. **66**, 2649 (1991).

[8] A. Koma, Surf. Sci. **267**, 29 (1992).

[9] E. J. Wanless and W. A. Ducker, Langmuir **13**, 1463 (1997).

[10] S. R. Forrest, Chem. Rev. **97**, 1793 (1997).

[11] J. A. Last, D. E. Hooks, A. C. Hillier, and M. D. Ward, J. Phys. Chem. B **103**, 6723 (1999).

[12] M. D. Ward, Chem. Rev. **101**, 1697 (2001).

[13] D. F. Evans and H. Wennerström, *The Colloidal Domain* (VCH Publishers, New York, 1994).

[14] K. A. Sharp, A. Nicholls, R. F. Fine, and B. Honig, Science **252**, 106 (1991).

[15] The potential parameters are taken from the CHARMM program. See the details at http://www.charmm.org.

[16] V. A. Parsegian and G. H. Weiss, J. Adhesion **3**, 259 (1972).

[17] J. Chun, J.-L. Li, R. Car, I. A. Aksay, and D. A. Saville (unpublished).

[18] J.-L. Li, J. Chun, N. S. Wingreen, R. Car, I. A. Aksay, and D. A. Saville, Phys. Rev. B **71**, 235412 (2005).

[19] M. Doi and S. F. Edwards, *The Theory of Polymer Dynamics* (Clarendon Press, Oxford, 1986).

[20] W. B. Russel, D. A. Saville, and W. R. Schowalter, *Colloidal Dispersions* (Cambridge University Press, New York, 1989).